

# Monitoring of indentation fracture and bending strain in $\alpha$ -SiC ceramics utilizing electrical response

A. KISHIMOTO\*

*Institute of Industrial Science, University of Tokyo, 7-22-1 Roppongi, Minato-ku, Tokyo 106-8558, Japan*

A. NAKAMICHI, Y. NAKAMURA

*Department of Applied Chemistry, Graduate School of Engineering, University of Tokyo, 7-3-1 Hongo, Bunkyo-ku, Tokyo 103-8656, Japan*  
*E-mail: kishim-a@ceram.iis.u-tokyo.ac.jp*

Propagation of indentation fracture was firstly monitored on  $\alpha$ -SiC ceramics through a current drop accompanied by the decrease in current conduction area. The current decrease ratio before and after indentation during the constant voltage application was proportional to the crack area formed. However, during the indentation, the current anomalously increased even though the indentation crack propagated. This phenomena is probably due to the piezoresistance effect which has already reported in SiC single crystal. When bending stress was applied to  $\alpha$ -SiC ceramics, the current increase ratio was proportional to the bending strain. A fracture foreseeing system is proposed for  $\alpha$ -SiC ceramics in which initial crack monitoring without stress application and bending strain monitoring utilizing the piezoresistance effect are combined. © 1999 Kluwer Academic Publishers

## 1. Introduction

To improve the reliability is the most important factor when ceramic is used as structural material. In practice, it is necessary to evaluate the mechanical property of ceramics and to grasp the crack propagation property. Furthermore, it is also desired to foresee a catastrophic fracture of a ceramic part during the operation, which should be based on the precise detection of fracture controlling flaw and strain. For these purposes, electric response could be utilized. Compared with optical observation, electric measurement is simple because, for visible crack area determination on opaque material, the cracked material should be fractured along the crack.

We have already reported a real time monitoring of indentation fracture in CuO ceramics [1]. Based on this result, identical monitoring of indentation fracture was performed on  $\alpha$ -SiC ceramics which is semiconductive as well as a representative structural ceramics. Apart from such damage estimation through the monitoring of fracture controlling flaw, bending strain was tried to be monitored through a conduction change probably due to the piezoresistance effect in SiC ceramics.

## 2. Experiments

### 2.1. Monitoring of indentation fracture in SiC ceramics

Commercial SiC ceramics (JIS; Japanese Industrial standard, supplied from Nihon Gaish, Co. Ltd., Japan)

were employed as test bars, which are hexagonal  $\alpha$ -SiC with density of 3.08 g/cm<sup>3</sup>. As received sample ceramics was first cut into bars with predetermined width (1.5 mm). After fixed in a resin (Castoglas resin, Buehler, Germany), sampled bars were sliced with thickness of 1.0 mm. Indentation surfaces were finished with diamond paste and silver pastes were attached as electrodes on the finished side. The final sample configuration is illustrated in Fig. 1. Current change during constant voltage (1 V) application was monitored when Vickers indentation was conducted for 30 s with load of 49, 98, or 196 N using a Hardness tester (HSV-20, Shimadzu, Japan).

### 2.2. Measurement of stress effect on electric conduction of SiC ceramics

Effects of mechanical stress were examined on electric resistance for SiC ceramics, where a conventional autograph (SV-950, Marubishi Co. Ltd., Japan) was used. First, on rectangular sample bars (3 × 0.7 × 18 mm<sup>3</sup>) prepared similar to the previous section, tensile stress was increased at a constant rate, hold, then decreased. During such process, electric current was monitored while a electric field was applied parallel to the stress direction. Stress effect perpendicular to the electric field was similarly examined. Sample setup is illustrated in Fig. 2a and b.

\* Author to whom all correspondence should be addressed.

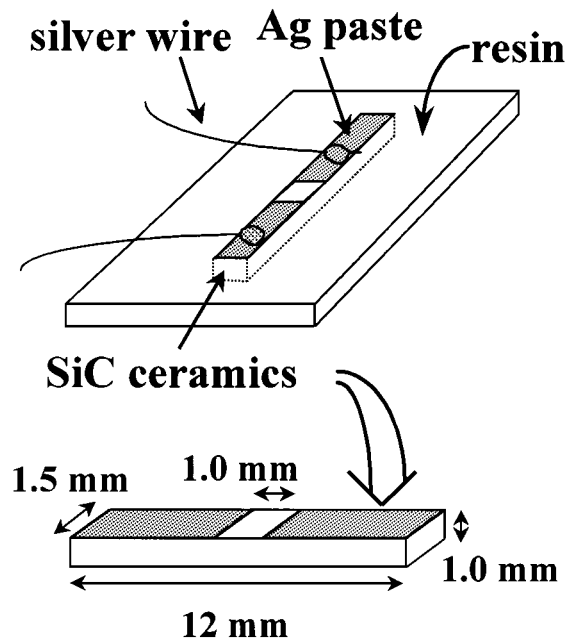


Figure 1 Sample configuration for monitoring of indentation fracture.

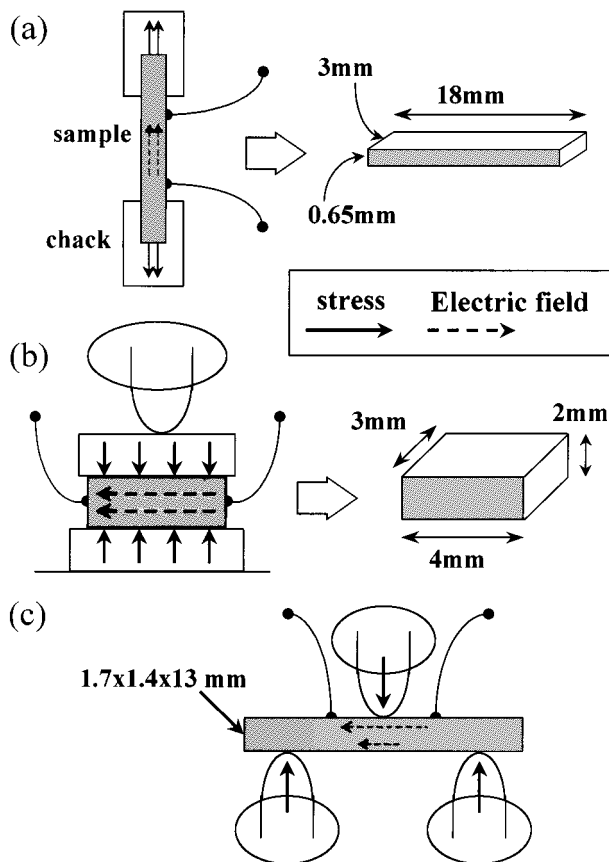


Figure 2 Sample setups for tension (a), compression (b) and bending (c) stress monitoring.

### 2.3. Monitoring of bending strain

Bending strain was monitored using the piezoresistance effect examined in the previous section. Commercial SiC ceramics were cut into bar ( $1.7 \times 1.4 \times 13 \text{ mm}^3$ ) and their indentation surface as well as the opposite sides were finished with diamond paste. Almost at the center of the finished surfaces, indentations were conducted with load of 9.8, 24.5, 49, 98 and 196 N. Two

electrodes (Ag paste) were attached on the opposite side of the indentations and constant voltage (1 V) was applied between the electrode during monitoring. Each sample bar with electrodes and a indentation mark was put on supports (10 mm span) so as to make the indented side down and bending load was applied at the center of the electrodes. The sample setup is illustrated in Fig. 2c. During this process, current change was monitored with the electrometer.

## 3. Results and discussions

### 3.1. Monitoring of indentation fracture

Fig. 3 illustrates the time-electric current curves obtained in the monitoring with load of 196 N. Electric current jumped substantially as soon as indentation starts, then remain constant during indentation. On unloading, current descendent to a small value which is lower than the initial value before indentation. Indentation monitoring for CuO ceramics is illustrated in Fig. 4 [1]. There are two step wise drops which are corresponding to crack propagation indentation onset and unloading, respectively. Such two steps crack propagation on indentation has already reported on transparent ceramics [2]. Contrary to CuO case, current increase was observed during indentation, which is probably due to the piezoresistance effect in SiC [3–6]. Current

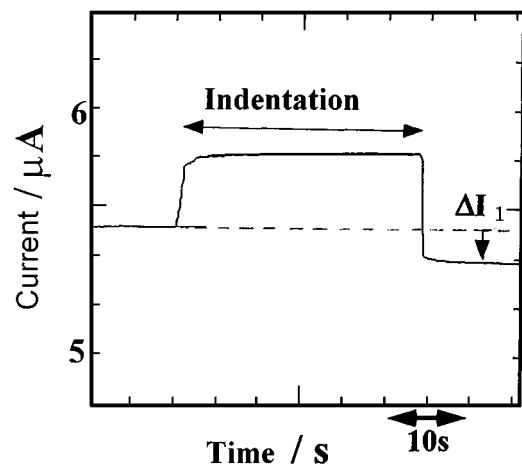


Figure 3 Time-current curves accompanied by indentation on SiC ceramics with load of 196 N.

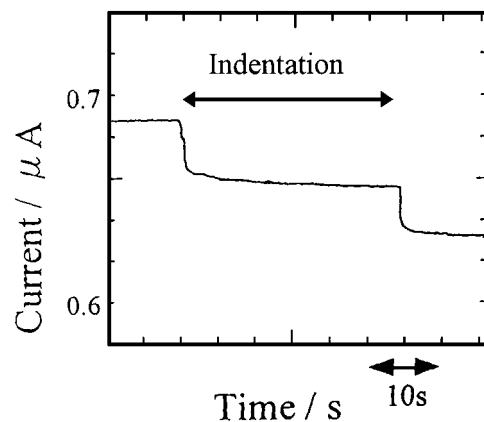


Figure 4 Time-current curves accompanied by indentation on CuO ceramics with load of 98 N [1].

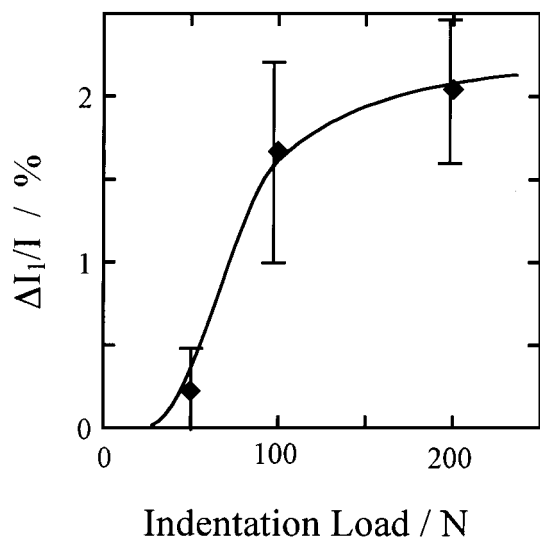


Figure 5 Dependence of fractional decrease in current on indentation load.

difference before and after indentation is thought to be caused by the crack propagation because current conducting area decreases accompanied by crack increases. In SiC ceramics, indentation fracture should proceed with similar manner to other ceramics, i.e., crack propagates both indentation onset and unloading. However, the piezoresistance effect is comparable to conducting area decrease, then the crack propagation can not be detected by electric conductions.

The decrease in current and the fractional decrease in current were defined as  $\Delta I_1$  and  $\Delta I_1/I$ , respectively. Fig. 5 shows the dependence of the fractional decrease in current on indentation load. As indentation load increase,  $\Delta I_1/I$  increases. Considerable scattering in  $\Delta I_1$  can be seen between samples even with the same load indentation, which is probably due to the difference in crack figure affected by the microstructure of SiC. In the present samples, cracked area can not optically be determined, however, which should directly related to  $\Delta I_1/I$  like CuO case [1]. When the indentation load was smaller than 24.5 N, current decrease cannot be detected. In such cases, indentation crack had not grown well in any direction.

### 3.2. Measurement of piezoresistance effect in $\alpha$ -SiC ceramics

The  $\alpha$ -SiC ceramics demonstrated a clear, reproducible stress sensitive resistivity change even though it is polycrystal. In the previous section the current change due to the piezoresistance effect seems to be related to the load applied. Then it can be utilized to a self-monitoring of applied stress in SiC ceramics.

It is widely known that SiC single crystal exhibits a piezoresistance effect, which is tried to be utilized in various fields [3–5]. However, there are few reports concerning the piezoresistance effect in SiC polycrystal. Hexagonal  $\alpha$ -SiC single crystal possesses independent six piezoresistance coefficients which has already measured [3]. The piezoresistance coefficients for polycrystal are thought to be different from those of single

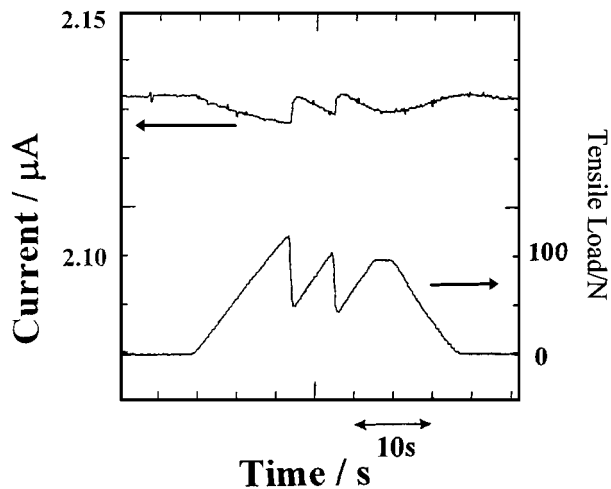


Figure 6 An electric current change under a constant voltage when stress is applied parallel to the electric field.

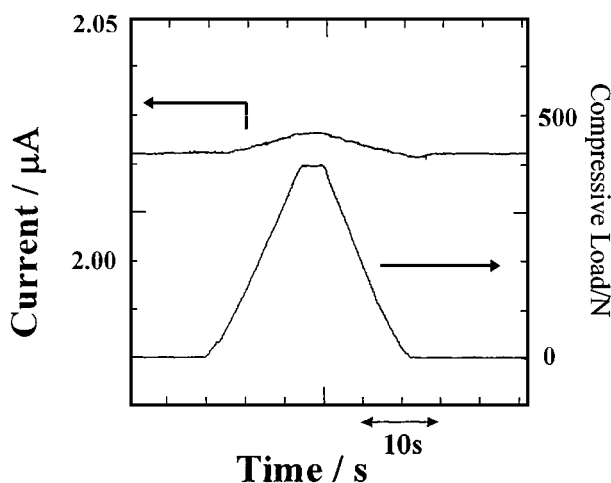


Figure 7 An electric current change under a constant voltage when stress is applied vertical to the electric field.

crystal because polycrystal consists of grain boundary and grain randomly oriented. Then the effect of stress parallel or vertical to the electric field on electric resistance were measured.

Fig. 6 illustrates a electric current change under a constant voltage when stress is applied, hold, and released parallel to the electric field. The coefficient of electric conduction change is negative to the stress applied and almost linearly related. Fig. 7 shows the result when stress is applied vertical to the electric field. The electric conduction change is almost linear to the applied stress. The coefficient of conduction change is positive to the compressive stress, that is, negative to the tensile stress, which is the same as the parallel stress application. The current recovered to the initial level when applied load was released from the sample.

From these results piezoresistance coefficients parallel ( $\pi_{para}$ ) and vertical ( $\pi_{ver}$ ) stress application were calculated to be  $4.2 \times 10^{-11}$  and  $6.5 \times 10^{-11}$   $m^2/N$ , respectively. The latter is a little larger than the former, however, both of them are in the same order. Taking into account of  $\pi_{para}$ ,  $\pi_{ver}$  and the geometry of Vickers indenter, resistance decrease on indentation is combined results from the piezoresistance effects derived from

the compressive stress both vertical and parallel to the electric field.

### 3.3. Monitoring of bending strain

Fig. 8 illustrates a electric current change when bending stress is applied on SiC ceramics indented with load of 9.8 N. As the applied load increases, the current increases, then suddenly drops at around 70 N, corresponding to the catastrophic total fracture.

Then current change on loading turned from positive to negative when both electrodes were replaced to the opposite side of loading. It is well known that tensile strain is generated on the opposite side of loading while compressive strain is generated on the loading side. Such strain of rectangular sample under bend loading is schematically illustrated in Fig. 9. Since both strain rates are almost the same in absolute value, the piezoresistance effect would have been canceled between tensile and compressive sides. The current density becomes large at the vicinity of loading surface when both electrodes are attached on the surface. When the electrodes are attached to the opposite side of loading, the current density of this side becomes large. As a

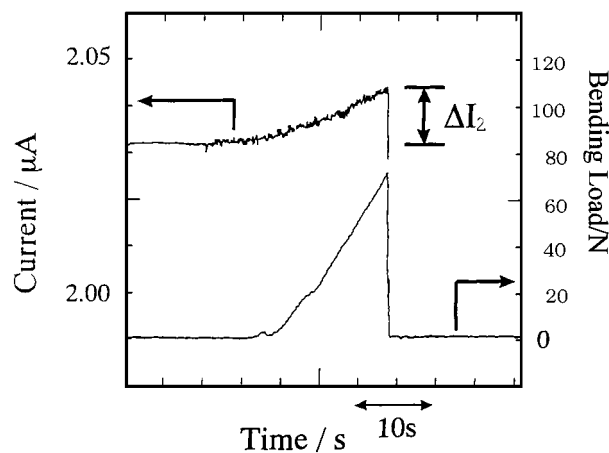


Figure 8 Time-current curves accompanied by bending fracture of SiC ceramics.

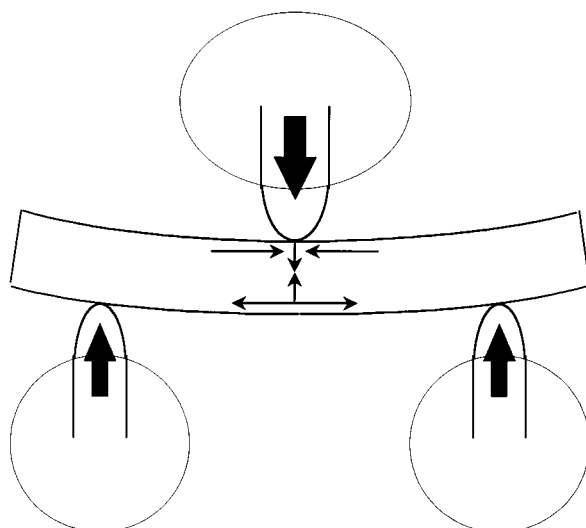


Figure 9 Schematic illustration of stress direction on bending.

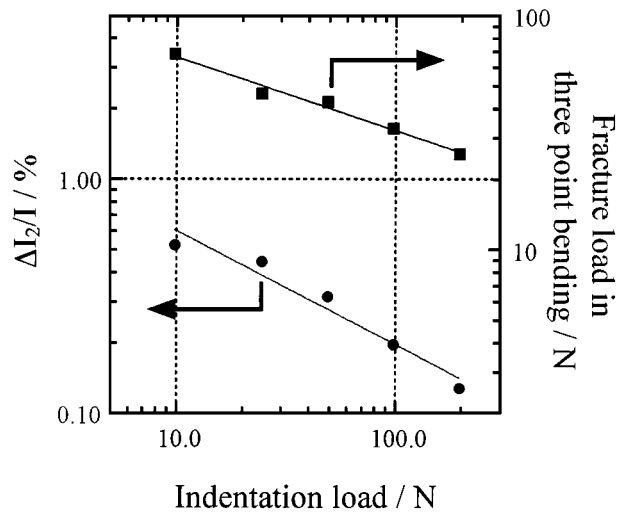


Figure 10 Dependence of fractional increase in current up to fracture and fracture load on indentation load.

result, the piezoresistance effect only for the electrode side was monitored on bending. Current increase rate of loading side electrodes condition is a little larger than the other condition. It is probably the vertical compressive stress contributes the current increase. In practice, larger current change is favorable for stress detection, then the electrodes were attached to the loading side.

The current change up to the fracture is defined as  $\Delta I_2$ , and current change ratio is also defined as  $\Delta I_2 / I$  ( $I$ ; current before loading). Fracture load and current decrease ratio are plotted against the indentation load as Fig. 10. The fracture load is inversely proportional to power to 1/3, which accord with experimental rule [7] as,

$$K_{IC} = 0.59 \left( \frac{E}{H} \right)^{1/8} (\sigma_f P^{1/3})^{3/4} \quad (1)$$

where  $K_{IC}$  is fracture toughness,  $E$  is the Young's module,  $H$  is hardness,  $\sigma_f$  is fracture stress, and  $P$  is indentation load. The relationship between current change and indentation load is different, i.e., the slope of  $\Delta I_2 / I$  vs indentation load is larger compared with the fracture load vs indentation load relation. This result indicates that piezoresistance coefficient slightly increase with indentation load. This is probably due to the decrease in real thickness accompanied by indentation crack propagation.

Based on the linear fracture mechanics, fracture stress is related to the fracture initiating crack length ( $c$ ) with the following expression [8],

$$\varepsilon_f E = \sigma_f = \frac{K_{IC}}{Y \sqrt{c}} \quad (2)$$

where  $\varepsilon_f$  is the fracture strain and  $Y$  is the figure constant of the crack.

When a large fracture initializing crack is introduced to a SiC ceramic part, fracture stress as well as fracture strain can be estimated from conduction change without loading before and after damage. This fracture stress can be converted to the conduction change up to fracture during loading using piezoresistance coefficient taking into account of initial crack length. Catastrophic

fracture can be prevented by stop the operation judging from the conduction monitoring.

#### 4. Conclusions

Conduction change accompanied by crack formation and strain were examined for SiC ceramics which is a representative structural ceramics as well as semi-conductive ceramics. Indentation crack length can be determined by the conduction change before and after indentation. Bending strain can be monitored by the conduction change probably due to the piezoresistance effect of SiC. Catastrophic fracture can be prevented by combining these two conduction changes, one between initial and damaged and the other during straining.

#### References

1. A. NAKAMICHI, A. KISHIMOTO and Y. NAKAMURA, *J. Mater. Sci. Lett.* **14** (1998) 249.

2. R. F. COOK and G. M. PHARR, *J. Amer. Ceram. Soc.* **73** (1990) 787.  
3. I. V. RAPATSKAYA, G. E. RUDASHEVSKII, M. G. KASAGANOVA, M. I. ISLITSIN, M. B. REIFMAN and E. F. FEDOTOVA, *Sov. Phys. Solid State* **9**(10) (1968) 2833.  
4. JOSEPH S. SHOR, LEALA BEMIS and ANTHONY D. KURTZ, *IEEE Transactions on Electron Devices* **41**(5) (1994) 145.  
5. ROBERT S. OKOJIE, ALEX A. NED, ANTHONY. D. KURTZ and WILLIAM N. CARR, *Transducers 91, Int. Conf. Solid-State Sens. Actuators (IEEE, IEEE Service Center, Piscataway, NJ, USA, IEEE, cat. no. 91CH2817, 5, 1991) p. 912.*  
6. TOSHIO HOMMA, KIICHI KAMIMURA, HAO YI CAI and YOSHINOBU ONUMA, *Sensors and Actuators A* **40** (1994) 93.  
7. P. CHANTIKUL, G. R. ANTIS, B. R. LAWN and D. B. MARSHALL, *J. Amer. Ceram. Soc.* **64** (1981) 539.  
8. G. R. IRWIN, "Handbuch der Physik," Vol. 6 (Springer Verlag, Berlin, 1958) p. 551.

*Received 10 March 1998*

*and accepted 2 March 1999*